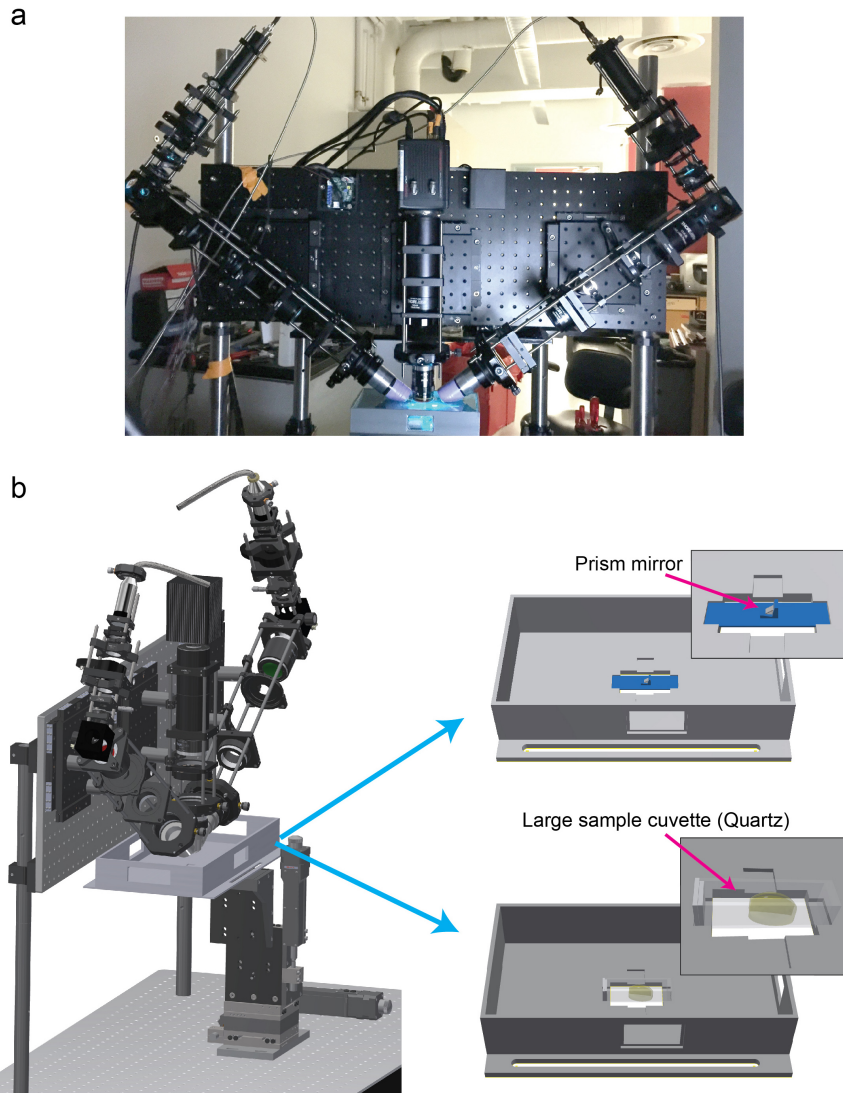
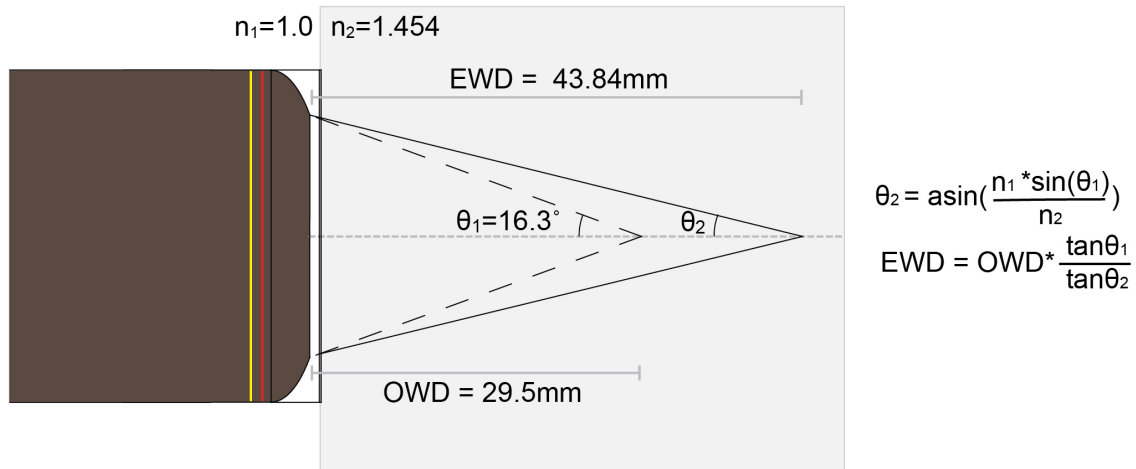


**Supplementary Figure 1. LSTM optical sectioning.** (a) x-z maximum intensity projections of an image stack acquired from a Human brain slice, shown in (b), stained with DAPI, with camera exposure times ranging from 0.1 to 1 millisecond in two different scanning modes (LSTM 1-AS and LSTM 2-AS). 2-AS mode allows for uniform planar illumination for achieving quantitative imaging. All scale bars are 100 microns. (b) LSTM imaging of a large thick section of cleared human brain tissue (~10.5mm x 14.1mm x 3mm) stained with DAPI. 0.5 ms exposure settings were used to acquire this dataset. Scale bar is 1 mm.

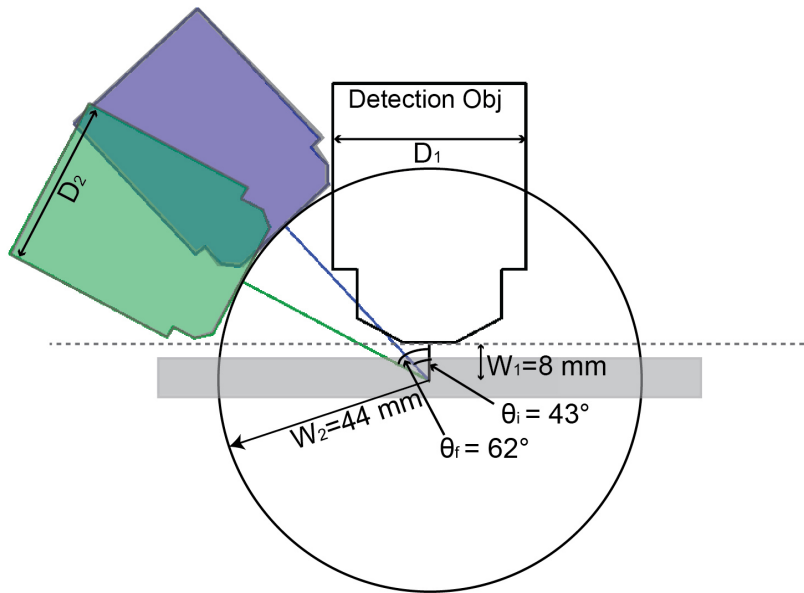


**Supplementary Figure 2. LSTM microscopy implementation.** (a) Picture of the physical LSTM microscope setup. (b) Side view of the 3D model of LSTM and the sample mounting system. The 3D printed sample chamber is designed to accommodate large biological samples while still allowing the objectives to be immersed in the immersion liquid. Two transparent glass windows, located on the lateral sides, facilitates positioning of the sample under the microscope. An additional window is realized at the bottom part of the chamber to allow illumination light to pass through. An adapter was used to mount a prism mirror at about  $10^\circ$  from the normal surface, to facilitate the optical alignment of the system.

a

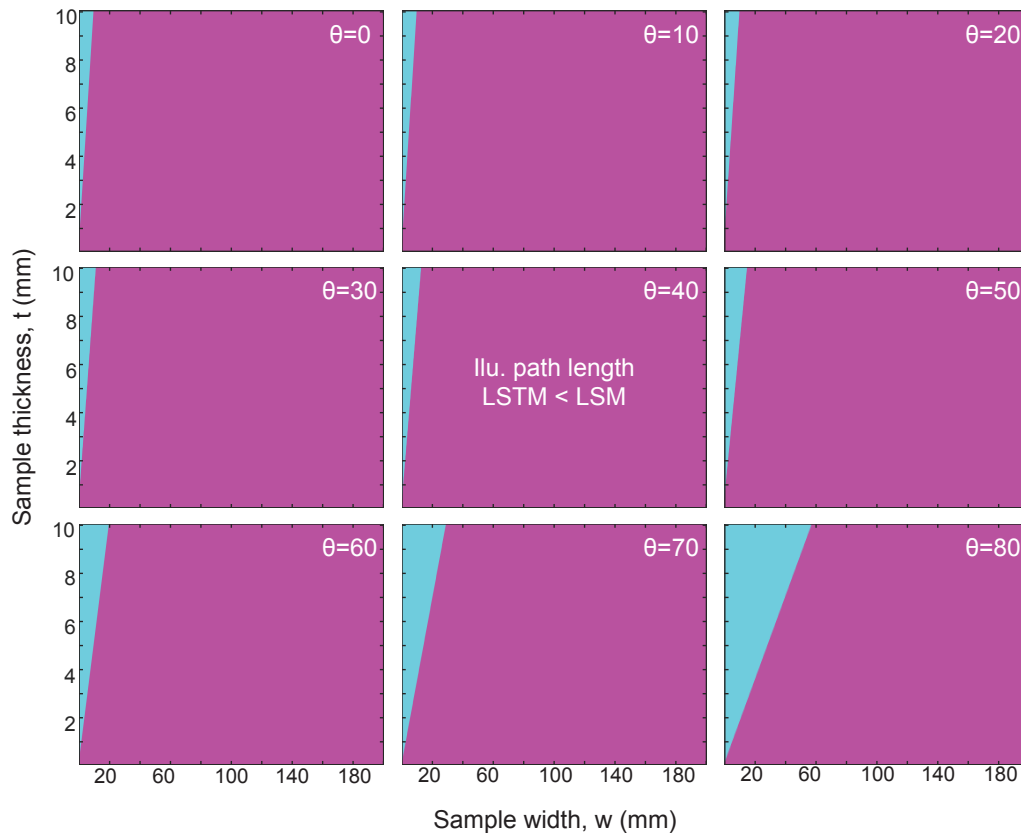


b

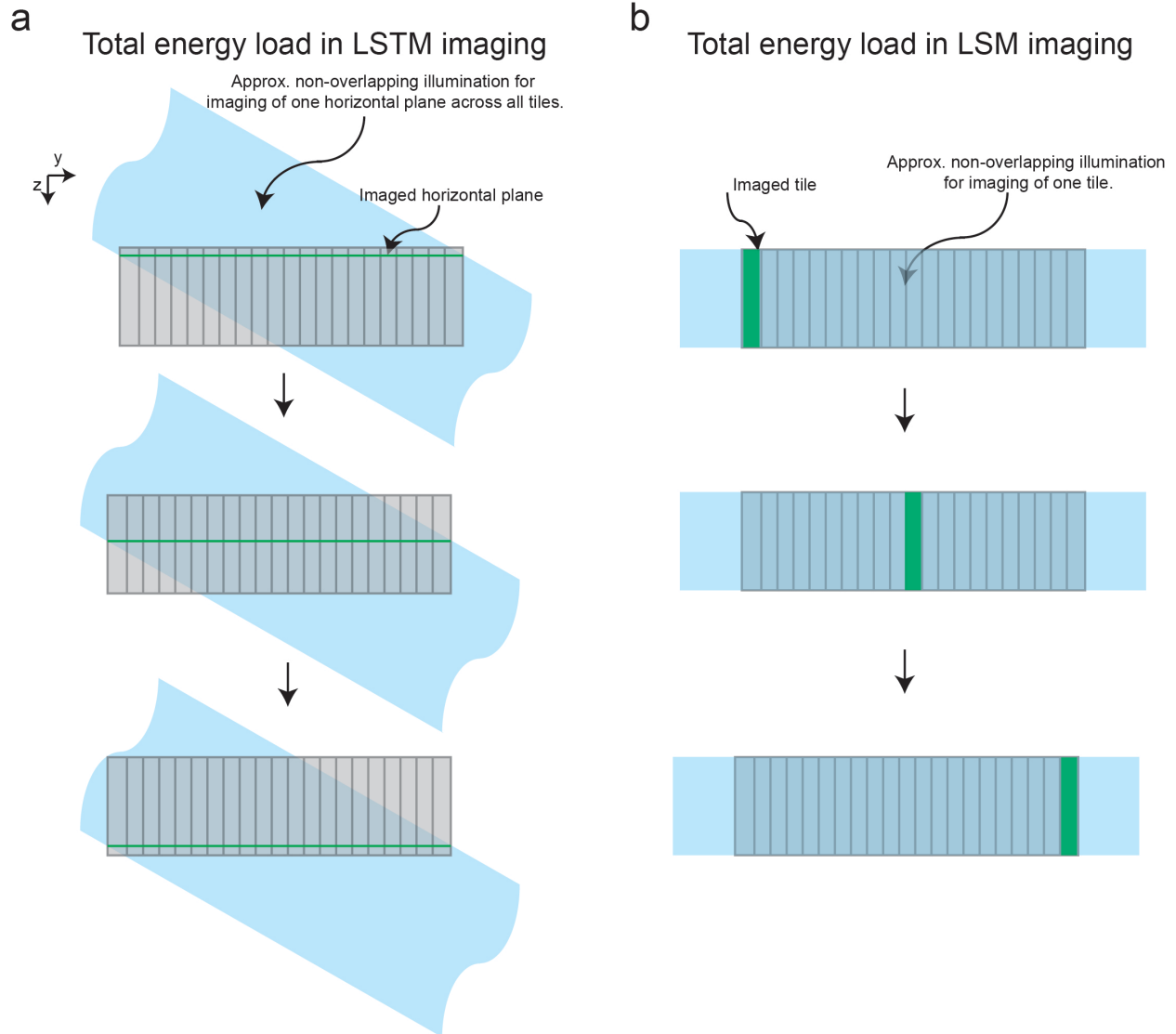


**Supplementary Figure 3. Geometric constraints of LSTM implementation.** (a) Schematics representing approximate calculations of the effective working distance (EWD) of the air illumination objective (Olympus Macro 4x/0.28NA/29.5WD Air) when used in immersion liquid (refractive index 1.454). Original working distance (OWD) is the working distance in air according to the objective specifications. A thin quartz coverslip and a 3D printed cap were used to seal the illumination objectives. EWD was estimated to be 43.84mm. (b) Geometric constraints calculation

for the co-arrangement of the illumination and detection objectives. The two boundary conditions are shown in blue and green shading of the illumination objective. For the upper bound limit (blue), the relationship among different parameters is defined by the equation  $W2 * \sin(\theta_i) = \frac{D1}{2} + D2 * \frac{\cos(\theta_i)}{2}$ . And the lower bound limit (green) by  $W2 * \cos(\theta_f) = W1 + D2 * \frac{\sin(\theta_f)}{2}$ .  $W1$  and  $W2$  are the effective working distance of detection and illumination objectives respectively.  $D1$  and  $D2$  are the diameters of the detection and illumination objectives respectively.  $\theta_i$  and  $\theta_f$  are the angular position of upper and lower bounds respectively. For Macro 4x/0.28NA/29.5mmWD as illumination objective and 10X/0.6NA/8mmWD as detection objective, the calculated  $\theta_i$  and  $\theta_f$  are  $43.32^\circ$  and  $63.37^\circ$  respectively. This range served as a starting point during the optical alignment of the system.



**Supplementary Figure 4. Comparison of illumination path lengths in LSTM and LSM.** The graphs compare the illumination path lengths required for imaging a sample of given width ( $w$ , the shortest lateral dimension) and thickness ( $t$ ). The ratios of illumination path lengths were calculated (using  $w/(\frac{t}{\cos(\theta)})$ ) for different angular arrangements and converted to a binary heat map. Magenta and Cyan regions mark the combinations of  $w$  and  $t$  for which the illumination path length was smaller in LSTM and LSM, respectively.



**Supplementary Figure 5. Total illumination energy load in LSTM vs. LSM.** The schematic summarizes the calculations of total energy loads imparted in LSTM and LSM for imaging of a sample of specific dimensions, imaged with a specific detection objective. (A) In LSTM, a horizontal plane across the entire sample is imaged with approximately non-overlapping thin sheets of light. Therefore, total energy load can be calculated by step-wise scanning of the sample (for each plane) through the illuminating light. For each of the step, all voxels that receive light are incremented by 1. The procedure was implemented of a range of parameters and two detection

objectives (10x/0.6NA/8mmWD and 25/1.0NA/8mmWD). (B) In LSM a stack (or tile) is acquired by approximately non-overlapping thin sheets of light. Total energy load is calculated by summing up illumination for all tiles in a row along the width. Note that the energy load for tiles along the sample length scales up by the same constant factor in LSTM and LSM, therefore we only simulated one row of tiles along the sample width.

### **Supplementary Videos.**

**Supplementary Video 1. Comparison of image volumes acquired with LSTM in 1-AS and 2-AS modes.** The 3D rendering visualizes the image stacks acquired from the same sample (human brain section stained with DAPI) with LSTM in 1-Axis Scan (1-AS) and simultaneous 2-Axes Scan (2-AS) mode.

**Supplementary Video 2. 3D model of LSTM implementation.** The 3D modelling and rendering was performed using Autodesk Inventor 2017, and the animation was performed using Autodesk Fusion 360 2017 and Matlab. The components labelled are LS (laser source), collimator, ND (neural density) filter mount, iris, ETL (electrically tunable lens), slit, CL (cylindrical lens), galvo scanner, SL (scan lens), iris and TL (tube lens)

**Supplementary Video 3. High-resolution LSTM imaging of intact *Thy1-eYFP* mouse central nervous system.** The bounding box for the entire sample is 11.8mm x 27.6 mm x 5.2 mm, and for the sub-volume shown is 5.1mm x 3.1mm x 3.5mm. The raw data was down-sampled 2x2 fold (to make the volume rendering feasible) for the sub-volume rendering.

**Supplementary Video 4. High-resolution LSTM imaging of a large tissue of *Thy1-eYFP* mouse brain.** The bounding box is 9.6mm x 13.5 mm x 5.34 mm. The raw data was down-sampled 4x4 fold to make the volume rendering feasible.

**Supplementary Video 5. Visualization of an image stack of vasculature stained rat brain tissue.** The Video visualizes an image stack acquired from a large rat brain slice (stained for vasculature with tomato lectin) using LSTM in 2-AS mode. The bounding box is 1mm x 1mm x 5mm.

**Supplementary Video 6. High-resolution LSTM imaging of a large expanded section of *Thy1-eYFP* mouse brain.** A thin (250 microns) coronal section was expanded ~4-fold using proExM procedure and imaged using LSTM with 10x/0.6NA detection objective. The resulting dataset (~6 TB) consisted of 723,300 full frame images (2048 x 2048). The data was down-sampled 8x8 fold to allow high-quality volumetric rendering.

**Supplementary Video 7. Rapid volumetric calcium imaging of highly motile Hydra.** GCaMP6s expressing Hydra was imaged using LSTM with 10x/0.6NA objective. Maximum intensity projections are shown for the two halves of the volume. First occurrences of longitudinal and radial contractions are annotated. Scale Bar is 100 microns.

**Supplementary Video 8. Neuronal activity traces of representative neurons.** Visualization of neuronal traces shown in **Figure 7b**.